



Discover Generics

Cost-Effective CT & MRI Contrast Agents

 **FRESENIUS
KABI**

[WATCH VIDEO](#)

AJNR

Comprehensive Review of Inner Ear Anatomy on Photon Counting CT

Dinesh Rao, John V. Murray, Amit K. Agarwal, Sukhwinder Johnny Sandhu and Pat A. Rhyner

AJNR Am J Neuroradiol published online 11 July 2024

<http://www.ajnr.org/content/early/2024/07/09/ajnr.A8410>

This information is current as of June 8, 2025.

Comprehensive Review of Inner Ear Anatomy on Photon Counting CT

Dinesh Rao¹, John V. Murray¹, Amit K. Agarwal¹, Sukhwinder Johnny Sandhu¹, Pat A. Rhyner¹

ABSTRACT

The inner ear contains many fissures and canals which can mimic pathology. Photon counting CT allows greater spatial and contrast resolution of these structures over traditional energy integrating CT detectors. Small channels containing nerves, arteries, and normal anatomy such as the cochlear cleft, cochlear and vestibular aqueducts are commonly encountered on temporal bone imaging. The improved visualization of these structures poses challenges for radiologists who are new photon counting CT. This manuscript updates the existing temporal bone anatomy literature with a detailed anatomical review of the inner ear and major nerves frequently encountered when reviewing temporal bone imaging.

ABBREVIATIONS: EID = energy-integrating detector; PCT = photon-counting computed tomography, CPA = cerebellopontine angle; IAC = internal auditory canal

Received month day, year; accepted after revision month day, year.

From the Department of Radiology (DR), (JVM), (AKA), (SJS), (PAR), Mayo Clinic, Jacksonville, FL, USA.

The authors have no disclosures

Please address correspondence to Dinesh Rao, MD, Department of Radiology, Mayo Clinic, 6500 San Pablo Blvd, Jacksonville, FL, 32224, USA: rao.dinesh@mayo.edu

INTRODUCTION

The inner ear contains many intrinsic and extrinsic fissures, and multiple channels which contain important anatomical structures. These structures have been described previously, and their recognition by radiologists is important to accurately interpret temporal bone imaging and to advise otologists for proper management of disease⁽¹⁻³⁾. Because of the linear appearance of these structures, they have been confused with fractures, and a lack of knowledge of these structures can lead to ignoring their presence

altogether. With recent advances in photon-counting computed tomography (PCT), resolution of temporal bone anatomy has become far greater than what was previously afforded by energy integrated detector (EID) CT scanners. The technical aspects of PCT have been reviewed and are beyond the scope of this anatomic review ^(4,5). The superiority of PCT over EID CT has been demonstrated particularly for small structures encountered in routine temporal bone imaging ^(6,7). Previously, the full extent of these structures was not visible, leaving portions of anatomy to be theoretical and visible only on pathological sectioning. As PCT has emerged, the fine detail of these structures is now routinely encountered. This review serves as an update to the existing literature by redefining these structures in greater resolution. All images contained in this review were acquired on a Siemens (Germany) NAEOTOM Alpha PCT scanner at 0.2 mm slice thickness.

MAIN BODY

The Inner Ear

The inner ear is located within the petrous bone. The otic capsule is the dense bone which surrounds the membranous labyrinth. The osseous labyrinth consists of the cochlea, vestibule, and semicircular canals [Figures 1 and 2]. The perilymphatic and membranous labyrinths are enclosed by the osseous labyrinth. The cochlea has 2.5 to 2.75 turns and spirals around the thin osseous modiolus from the wider base to the narrow apex. The basal turn of the cochlea is separated from the middle ear by the cochlear promontory. The spiral lamina projects from the modiolus into the cochlear canal and divides it into the scala vestibuli and scala tympani. The scala vestibuli and tympani contain perilymph. The scala media, also called the cochlear duct, contains endolymph, and is separated from the scala vestibuli by Reissner membrane. The scala vestibuli and tympani communicate with each other at the apex of the modiolus called the helicotrema. Vibration from sound enters the scala vestibuli via the oval window and exits the scala tympani via the round window. The round window and scala tympani are typically the sites for cochlear implant insertion.

The perilymph cavity of the cochlea is continuous with the vestibule posteriorly. The vestibule is an ovoid structure posterolateral to the cochlea connecting to the superior, posterior and lateral semicircular

canals. The oval window is located at the anterolateral aspect of the vestibule. The semicircular canals are oriented orthogonal to each other. Each canal has a bulbous dilatation called an ampulla which houses the vestibular sense organ containing hair cells. The non-ampullary superior end of the posterior semicircular canal and the posterior end of the superior semicircular canal are fused into a common crus. The arcuate eminence is an osseous ridge above the superior semicircular canal on the anterior surface of the petrous bone and serves as the posterior boundary of the middle cranial fossa. A wide range of symptoms including sound induced vertigo, or Tullio phenomenon, can be caused by dehiscence of the superior, or less commonly, other third window abnormalities ⁽⁸⁾.

The fissula ante fenestram (FAF) is a small extension of the perilymphatic space that is obliterated with connective tissue. Histopathologically, the FAF appears as a cleft located anterior to the oval window and medial to the cochleariform process. In our experience, the normal FAF is not well visualized on PCT. The area around the FAF is believed to be the usual origin of fenestral otosclerosis. [Figure 1d]. The cochlear cleft is located anterior to the FAF and should not be confused for otosclerosis ^(3,9). The cochlear cleft is hypothesized to be related to incomplete ossification of development of the otic capsule, containing bone marrow and fat lobules which account for the low density. The cochlear cleft is thinner and linear and can follow the curvature of the medial aspect of the cochlea [Figure 1e].

The cochlear aqueduct, containing perilymph, is funnel shaped and located just inferior to the internal auditory canal (IAC), extends from the basal turn of the cochlea as a narrow slit and widens to the medial surface of the petrous bone where it drains into the subarachnoid space. The lateral orifice is near the round window, traditionally beyond the resolution of EID CT, although it may be visible on PCT images [Figure 1f].

The vestibular aqueduct which contains the endolymphatic duct and sac originates along the posterolateral border of the vestibule and passes posterior and superior to the common crus, turns inferiorly and posterior to the posterior semicircular canal, finally opening into the posterior aspect of the petrous bone. While the larger posterior part of the vestibular aqueduct is visible on EID CT scans, the more anterior origin is visible on PCT [Figure 2e].

Major Nerves

There are five intratemporal segments of the facial nerve: canalicular, labyrinthine, geniculate, tympanic, and mastoid [Figure 3 a-f]. The canalicular segment is contained within the anterior superior part of the IAC. The labyrinthine segment enters the temporal bone just above the cochlear nerve. The labyrinthine segment is the shortest segment, measuring 3 to 4 mm in length.

The geniculate segment contains the geniculate ganglion which gives off 3 major branches. The greater superficial petrosal nerve contains preganglionic parasympathetic fibers, providing innervation to the lacrimal gland, nasopharynx, soft palate and some sensory taste fibers from the soft palate. [Figure 3b]. The external petrosal nerve courses on the petrous ridge's anterior surface ⁽¹⁰⁾. It carries sympathetic fibers surrounding the middle meningeal artery. In our experience, this cannot be visualized on PCT. The lesser petrosal nerve, a branch of the glossopharyngeal nerve also called the small superficial petrosal nerve, contains a small branch from the geniculate ganglion. The nerve passes from the geniculate ganglion to the floor of the middle cranial fossa and exits through foramen ovale to provide parasympathetic fibers to the parotid gland.

From the geniculate segment, the facial nerve turns posteriorly and laterally forming the first genu. The facial nerve is situated superior to the cochlear promontory and travels posteriorly in the tympanic segment. The tympanic segment runs inferior to the lateral semicircular canal and superior to the oval window and stapes footplate. Very thin bone encapsulating the tympanic portion of the facial nerve may be variably present or absent. When present, the thin bone is more often visualized with PCT due to higher spatial resolution ⁽⁶⁾. The facial nerve then enters the mastoid bone and turns inferiorly at the second genu exiting the skull base through the stylomastoid foramen and enters the parotid gland. The nerve to the stapedius muscle is given off by the facial nerve behind the pyramidal eminence. The chorda tympani originates from the lateral border of the descending mastoid segment and ascends through a recurrent course into the middle ear cavity through the canaliculus of the chorda tympani [Figure 4 a, b and c]. The nerve crosses the inner surface of the tympanic membrane, passing between

the long process of the incus and manubrium above the tensor tympani tendon. The chorda tympani departs the tympanic cavity in the medial aspect of the petrotympanic fissure and exits the skull base through the anterior tympanic aperture [Figure 4d].

The vestibulocochlear nerve arises from the lateral aspect of the pons, extends through the cerebellopontine angle (CPA), enters the IAC and divides into the anterior cochlear nerve and posterior vestibular nerves which are further divided into superior and inferior divisions ⁽¹¹⁾. The cochlear nerve enters the basal turn of the cochlea through the cochlear aperture, providing sensory innervation to the organ of Corti. The superior vestibular nerve division travels through the superior posterior aspect of the IAC and extends through a narrow osseous channel to innervate the superior and lateral semicircular canals and their respective ampullae, as well as the utricle and saccule. The inferior division passes through the inferior posterior IAC and subdivides into the singular [Figure 6] and saccular nerves which provide innervation to the ampulla of the posterior semicircular canal and saccule respectively. Singular neurectomy has been used to treat intractable benign positional vertigo ⁽¹²⁾.

Arnold's nerve, also known as the auricular branch of the vagus nerve, arises from the lateral margin of the pars vascularis of the jugular foramen, travels through the mastoid canaliculus and joins the facial nerve mastoid segment inferior to the nerve to stapedius [Figure 5]. It supplies pain fibers to the posterior external auditory meatus and auricle and is one of the potential etiologies of referred otalgia. Arnold's nerve is formed primarily from the superior ganglion of the vagus nerve, with a small contribution from the glossopharyngeal nerve. Arnold's nerve contains paraganglia and are a site of paragangliomas which occur within the jugular foramen and can erode the skull base. It is also considered the origin for the rare primary paraganglioma of the facial canal ^(13, 14).

Jacobson's nerve is the tympanic branch of the glossopharyngeal nerve. It arises from the inferior glossopharyngeal ganglion and enters the skull base at the inferior tympanic canaliculus [Figure 7] ⁽¹⁵⁾. It courses within the inferior tympanic canaliculus in a coronal oblique fashion to the cochlear promontory where it forms the tympanic plexus. Tympanic paragangliomas (glomus tympanicum) originate from paraganglia along the tympanic nerve (Jacobson's nerve) at the cochlear promontory.

Paragangliomas may spread along Jacobson's nerve involving the jugular fossa and posterior wall of the carotid canal. Aberrant internal carotid arteries course through an expanded inferior tympanic canaliculus and must be differentiated from glomus tympanicum tumors which can appear similarly as a red pulsatile mass on otoscopic exam and can both be causes of pulsatile tinnitus.

The petromastoid canal, also called the subarcuate canaliculus, contains the subarcuate artery and vein which provides the vascular supply to the vestibule, semicircular canal and facial nerve ⁽¹¹⁶⁾. The artery arises from the anterior inferior cerebellar artery (AICA) and the vein drains into the superior petrosal sinus. The canal is in the superior portion of the petrous bone and passes in between the anterior and posterior crura of the superior semicircular canal extending between the posterior fossa and mastoid air cells [Figure 8].

Conclusion

Visualization of inner ear anatomy is much improved due to the advantages of PCT over EID CT. This allows for better characterization of many structures, such as the full extent of the vestibular and cochlear aqueducts and cochlear cleft, as well as many nerves and their anatomical relationships. This review serves as a new resource in which we hope sub-specialty and general radiologists will find helpful as PCT becomes more available to the radiology community.

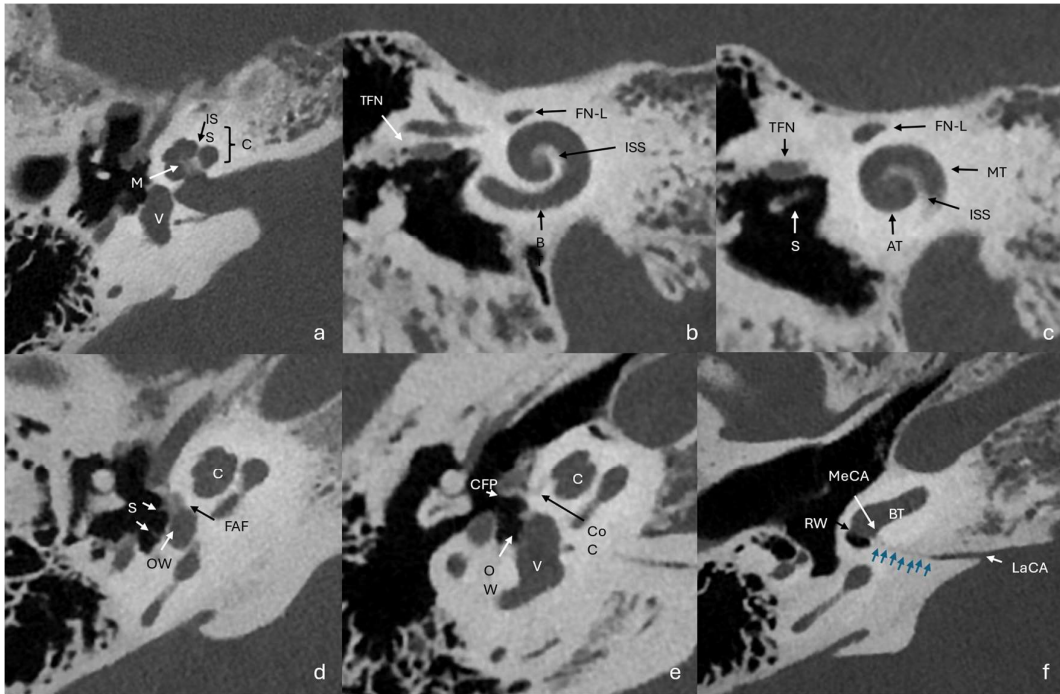


Figure 1 (a): axial image of the cochlea (C) and vestibule (V) : ISS: interscalar septum, M: modiolus. (b and c): Stenver's projection reconstructed images. BT: basal turn cochlea, LFN: labyrinthine segment facial nerve, TFN: tympanic segment facial nerve. (b): MT: middle turn cochlea, S: stapes. (d): Axial CT image demonstrating demineralized appearance of the fissula ante fenestram (FAF) anterior to the oval window (OW). The FAF is only visible in patients with otosclerosis. Note the expansile appearance and relative posterior position relative to the cochlear cleft (CC) in figure (e). Note the anterior and posterior crura of the stapes. (e): axial image of the cochlea and vestibule. CFP: cochleariform process. (f): axial image of the cochlear aqueduct. The cochlear aqueduct (blue arrows) is visible extending from the medial petrous ridge to the basal turn of the cochlea near the round window (RW). LaCA: lateral cochlear aqueduct orifice, MeCA: medial cochlear aqueduct orifice.

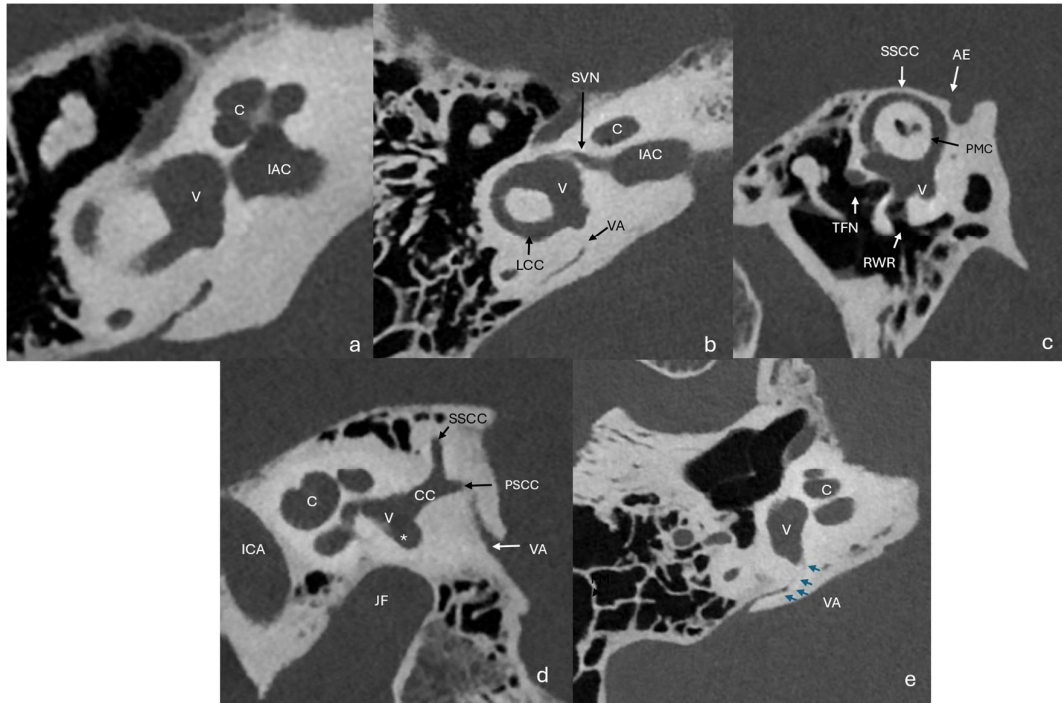


Figure 2 (a): axial image of the cochlea (C) and vestibule (V). IAC: internal auditory canal. (b): axial image of the vestibular structures. SVN: superior vestibular nerve, LCC: lateral semicircular canal, VA: vestibular aqueduct. (c): Poschl reconstructed image of the superior semicircular canal (SSCC). AE: arcuate eminence, PMC: petromastoid canal, RWR: round window recess, TFN: tympanic segment facial nerve. (d): sagittal image of the vestibular structures. CC: common crus of the superior and posterior semicircular canals, ICA: internal carotid artery, JF: jugular fossa, PSCC: posterior semicircular canal, VA: vestibular aqueduct, *: PSCC ampulla. (e): axial image of the vestibular aqueduct (blue arrows). PCT can demonstrate the anterior orifice in the vestibule. FM: facial nerve mastoid segment.

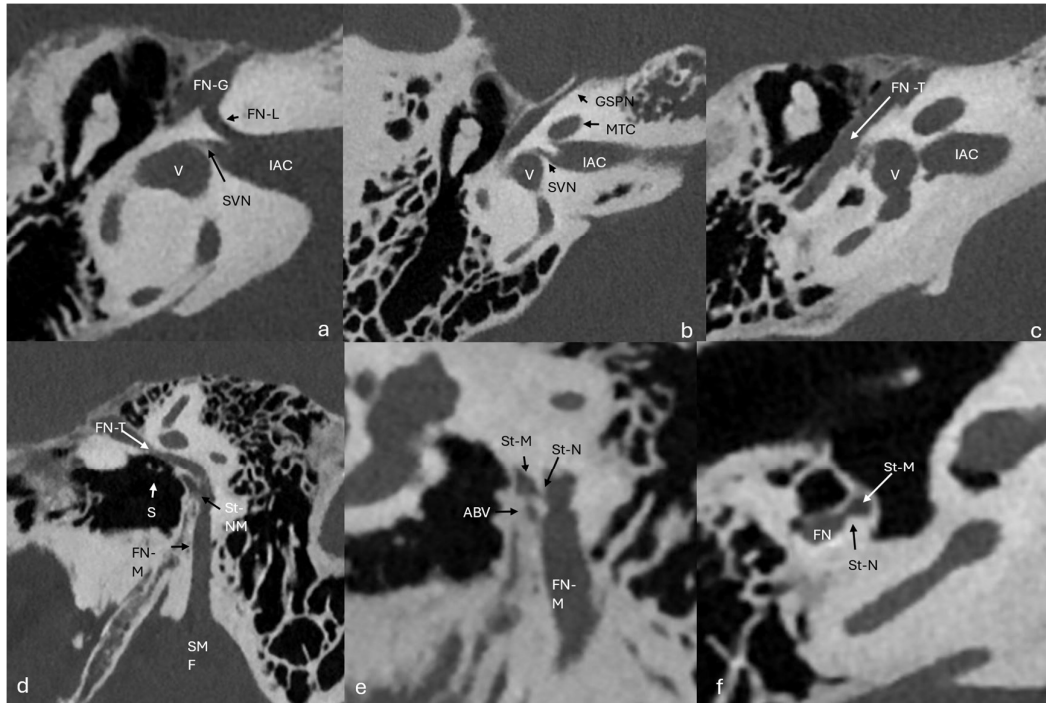


Figure 3 (a): axial image of the facial nerve including the labyrinthine segment (FN-L), geniculate fossa (FN-G) which contains the geniculate ganglion. Note the superior vestibular nerve (SVN) which exits the posterior internal auditory canal (IAC) to innervate the vestibular structures (V). (b): axial image of the greater superficial petrosal nerve (GSPN), MTC: middle turn cochlea. (c): axial oblique image of the tympanic segment of the facial nerve (FN-T). (d): sagittal oblique image demonstrating the relationship of the FN-T and mastoid segments (FN-M) with adjacent structures. Note the nerve to the stapedius muscle (St-N) and the FN-T position superior to the stapes (S). SMF: stylomastoid foramen. (e): Sagittal oblique image demonstrating the relationship of the FN-M, the auricular branch of the vagus nerve (Arnold's nerve) (ABV), and the stapedial nerve (St-N) and muscle (St-M). (f): axial oblique image demonstrating the St-N exiting the mastoid segment of the facial nerve (FN) and entering the St-M.

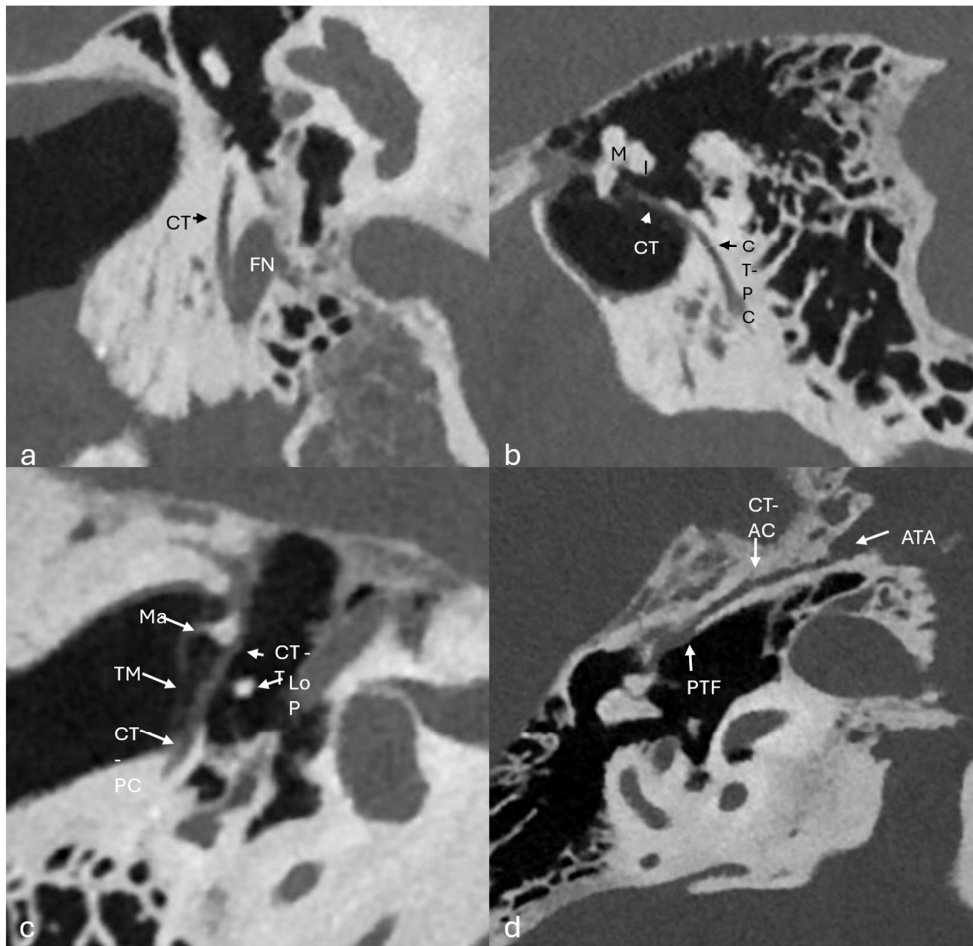


Figure 4 (a): Coronal oblique image of the chorda tympani origin (CT) from the mastoid segment of the facial nerve (FN). (b): Sagittal oblique image of the posterior canaliculus of the CT-PC extending through the mastoid bone and entering the middle ear cavity. Note the course adjacent to the malleus (M) and Incus (I). (c): axial oblique image of the tympanic segment (CT-T) medial to the tympanic membrane (TM). The nerve passes in between the manubrium of the malleus (Ma) and long process of the incus (LoP). (d): The anterior aspect of the CT exits the middle ear cavity through the medial aspect of the petrotympanic fissure (PTF), traveling through the anterior canaliculus (CT-AC), then exits the skull base at the anterior tympanic aperture (ATA) to join the lingual nerve.

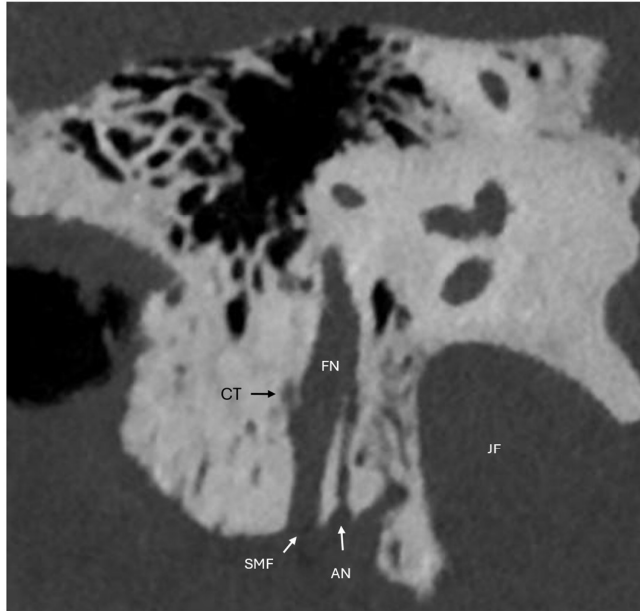


Figure 5: Coronal oblique image demonstrating Arnold's nerve (AN) as it originates from the lateral aspect of the jugular fossa (JF). AN enters the facial nerve canal (FN) mastoid segment. Note the origin of the posterior canalculus of the chorda tympani (CT) and the stylomastoid foramen (SMF).

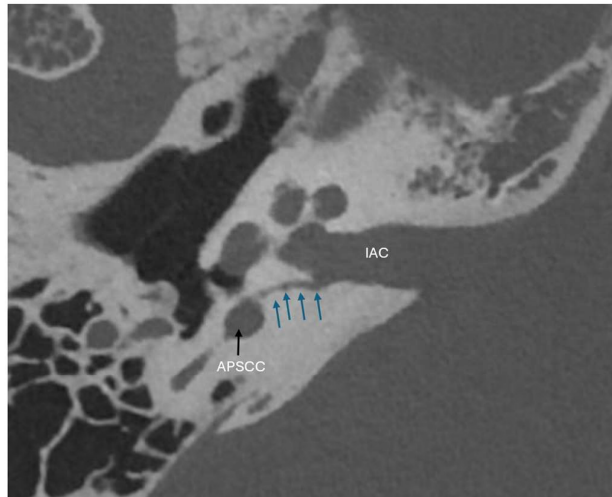


Figure 6: Axial image demonstrating the singular nerve arising from the inferior IAC and extending through the otic capsule into the ampulla of the posterior semicircular canal (APSC).

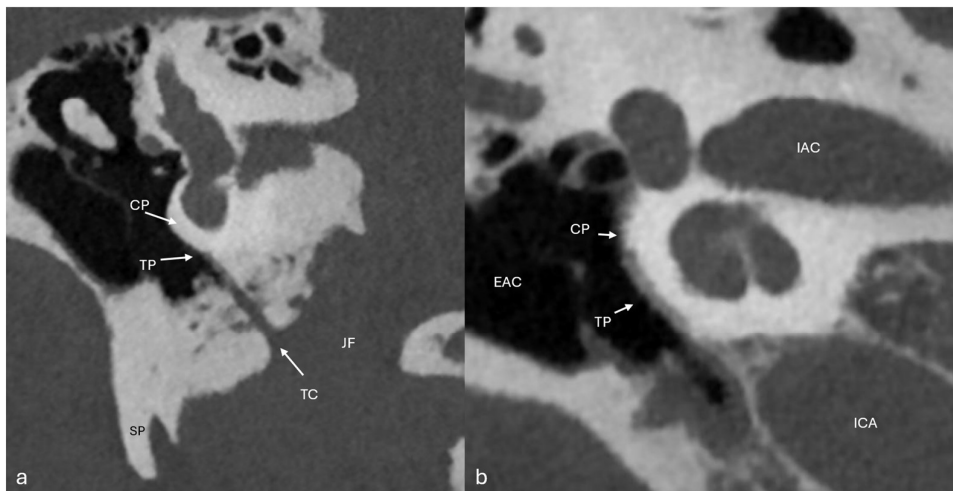


Figure 7 (a): Coronal oblique image of the course of Jacobson's nerve through the inferior tympanic canaliculus (TC) along the undersurface of the cochlear promontory (CP) where it forms the tympanic plexus (TP). JF: jugular foramen, SP: styloid process. (b):

Coronal oblique image demonstrating the TP along the CP. Note the position of the external auditory canal (EAC), internal auditory canal (IAC), and internal carotid artery (ICA) for orientation.

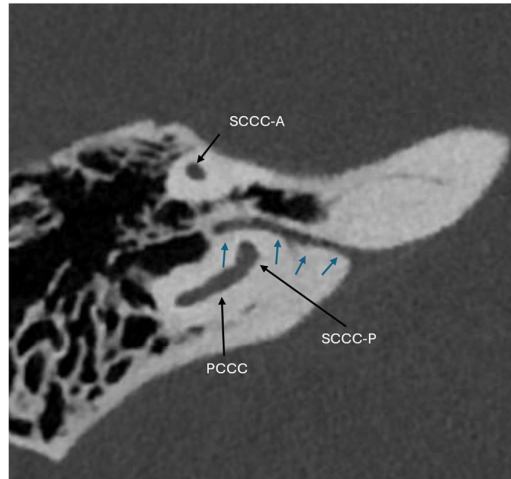


Figure 8: Axial image demonstrating the petromastoid canal (blue arrows) which contains the subarcuate artery and vein. The canal passes in between the superior semicircular canal anterior (SCCA-A) and posterior (SCCA-P) crura. Note the position to the posterior semicircular canal (PCCC).

REFERENCES

1. Moonis G, Ginat DT. Normal Anatomic Structures, Variants, and Mimics of the Temporal Bone. *Neuroimaging Clin N Am*. 2022 May;32(2):345-361. doi: 10.1016/j.nic.2022.01.007. PMID: 35526961.
2. Koesling S, Kunkel P, Schul T. Vascular anomalies, sutures and small canals of the temporal bone on axial CT. *Eur J Radiol*. 2005 Jun;54(3):335-43. doi: 10.1016/j.ejrad.2004.09.003. PMID: 15899333.
3. Chadwell JB, Halsted MJ, Choo DI, et al. The cochlear cleft. *AJNR Am J Neuroradiol*. 2004 Jan;25(1):21-4. PMID: 14729522; PMCID: PMC7974172.
4. Leng S, Bruesewitz M, Tao S, et al. Photon-counting Detector CT: System Design and Clinical Applications of an Emerging Technology. *Radiographics*. 2019 May-Jun;39(3):729-743. doi: 10.1148/rg.2019180115. PMID: 31059394; PMCID: PMC6542627.
5. Ferda J, Vendiš T, Flohr T, et al. Computed tomography with a full FOV photon-counting detector in a clinical setting, the first experience. *Eur J Radiol*. 2021 Apr;137:109614. doi: 10.1016/j.ejrad.2021.109614. Epub 2021 Feb 24. PMID: 33657475.
6. Hermans R, Boomgaert L, Cockmartin L, et al. Photon-counting CT allows better visualization of temporal bone structures in comparison with current generation multi-detector CT. *Insights Imaging*. 2023 Jul 3;14(1):112. doi: 10.1186/s13244-023-01467-w. PMID: 37395919; PMCID: PMC10317909.
7. Zhou W, Lane JI, Carlson ML, et al. Comparison of a Photon-Counting-Detector CT with an Energy-Integrating-Detector CT for Temporal Bone Imaging: A Cadaveric Study. *AJNR Am J Neuroradiol*. 2018 Sep;39(9):1733-1738. doi: 10.3174/ajnr.A5768. Epub 2018 Aug 9. PMID: 30093479; PMCID: PMC6128765.
8. Wackym PA, Agrawal Y, Ikezono T, et al. Editorial: Third Window Syndrome. *Front Neurol*. 2021 Jun 18;12:704095. doi: 10.3389/fneur.2021.704095. PMID: 34220698; PMCID: PMC8250852.
9. Pucetaite M, Quesnel AM, Juliano AF, et al. The Cochlear Cleft: CT Correlation With Histopathology. *Otol Neurotol*. 2020 Jul;41(6):745-749. doi: 10.1097/MAO.0000000000002637. PMID: 32221113.
10. Nageris B, Braverman I, Kalmanowitz M, et al. Connections of the facial and vestibular nerves: an anatomic study. *J Otolaryngol*. 2000 Jun;29(3):159-61. PMID: 10883829.
11. Anthony Zandian, R. Shane Tubbs, Marios Loukas, Chapter 25 - Anatomy of the Vestibulocochlear Nerve. Editor(s): R. Shane Tubbs, Elias Rizk, Mohammadali M. Shoja, Marios Loukas, Nicholas Barbaro, Robert J. Spinner, *Nerves and Nerve Injuries*, Academic Press, 015, Pages 365-370, ISBN 9780124103900.
12. Corvera Behar G, García de la Cruz MA. Surgical Treatment for Recurrent Benign Paroxysmal Positional Vertigo. *Int Arch Otorhinolaryngol*. 2017 Apr;21(2):191-194. doi: 10.1055/s-0037-1599784. PMID: 28382130; PMCID: PMC5375711.
13. Nadimi S, Leonetti JP, Marzo SJ, et al. Glomus faciale tumors: A report of 3 cases and literature review. *Ear Nose Throat J*. 2017 Mar;96(3):E7-E12. doi: 10.1177/014556131709600318. PMID: 28346648.
14. Mafee MF, Raofi B, Kumar A, Muscato C. Glomus faciale, glomus jugulare, glomus tympanicum, glomus vagale, carotid body tumors, and simulating lesions. Role of MR imaging. *Radiol Clin North Am*. 2000 Sep;38(5):1059-76. doi: 10.1016/s0033-8389(05)70221-9. PMID: 11054969.

15. Kanzara T, Hall A, Virk JS, et al. Clinical anatomy of the tympanic nerve: A review. *World J Otorhinolaryngol* 2014;4(4):17–22. <https://doi.org/10.5319/wjo.V4.i4.17>.
16. Akyol Y, Galheigo D, Massimore M, et al. Subarcuate artery and canal: an important anatomic variant. *J Comput Assist Tomogr* 2011;35(6):688–9.